SAND2000-1872C

MEMS-Vol. 2, Microelectromechanical Systems (MEMS):
ASME IMECE 2000
November 5-10, Orlando, Florida

Paper Number

DESIGN AND ANALYSIS OF A PRECONCENTRATOR FOR THE μCHEMLAB™

C. Channy Wong, Jeb H. Flemming

Engineering Science Center
Sandia National Laboratories
Albuquerque, NM 87185-0826

Ronald P. Manginell, Richard J. Kottenstette, Gregory C. Frye-Mason

Microsystems Center
Sandia National Laboratories
Albuquerque, NM 87185-1425

ABSTRACT

Preconcentration is a critical analytical procedure when designing a microsystem for trace chemical detection, because it can purify a sample mixture and boost the small analyte concentration to a much higher level allowing a better analysis. This paper describes the development of a micro-fabricated planar preconcentrator for the μChemLab™ at Sandia. To guide the design, an analytical model to predict the analyte transport, adsorption and desorption process in the preconcentrator has been developed. Experiments have also been conducted to analyze the adsorption and desorption process and to validate the model. This combined effort of modeling, simulation, and testing has led us to build a reliable, efficient preconcentrator with good performance.

NOMENCLATURE

- a adsorbent surface area per adsorbent volume
- c analyte concentration exiting PC
- c_{min} minimum breakthrough concentration
- c_o analyte concentration in the feed stream
- c_1 saturation concentration at an elevated temperature
- d adsorbent layer thickness
- h flow channel height
- k gas-phase mass transfer coefficient
- l adsorbent layer length
- q_o analyte concentration in the adsorbent bed
- q_f final analyte concentration in the adsorbent bed
- t load time during adsorption and desorption
- t_{sat} time to establish a saturation zone
- u average channel flow velocity
- u_{sat} propagation speed of the advancing saturation front in the adsorbent bed
- ε void fraction

INTRODUCTION

Front-end sampling with a preconcentrator is a critical processing step for the success of many micro-analytical detection systems. A preconcentrator (PC) can selectively collect, purify, and boost the concentration of the sample (target analyte) to improve the detection capability and to discriminate against interferants. At Sandia, we have designed, built, and tested a novel preconcentrator as part of a program to develop an autonomous micro-analytical system, μChemLab™ (Fig. 1). The μChemLab™ can detect and identify trace concentrations of target analytes even in the presence of interfering chemicals [1, 2].

Conventional preconcentrators consist of a small tube, usually 6 mm in diameter by 100 mm long, packed with adsorbent resins between two glass wool plugs. First, the desired analytes are collected on the resin by passing a sample mixture through the PC. Then these analytes are thermally desorbed and released into the gas stream as a plug of higher concentrated analytes for analysis. Many fold higher analyte

concentrations can be achieved in this way. Much effort has been devoted to develop micro-total analysis systems, however only limited work exists in developing miniaturized preconcentrators. One such effort is a microfabricated, electrochemical-based detection system developed at Stanford using an *electrochemical* preconcentrator [3, 4].

The present preconcentrator design is relatively different from the previous design and is built for gas sample collection. It is a micro-fabricated hot plate coated with a micro-porous adsorbent. The adsorbent is a surfactant templated (ST) sol gel tailored to the targeted analyte being collected. The adsorbent region is covered by a Pyrex lid that has an inlet and outlet port on the top (Fig. 2). Together these machined pieces form a flow channel. (The normal size of the channel is 2.8 mm wide, 3.8 mm long, and 150 μm.) During the sampling phase, flow will pass through the channel and target analyte will be collected on the sol-gel adsorbent. Next, during the analysis phase, the adsorbent will be rapidly heated by a thin-film Pt resistor (from room temperature to 200°C within 10 msec) to efficiently desorb the target analyte back into the carrier gas stream for separation and detection.

FABRICATION AND ASSEMBLY

The micro-hot plate part of the PC is fabricated by through-wafer silicon etching (via the Bosch process), stopping on a low-stress silicon nitride membrane layer. Prior to silicon etching, a thin-film Pt heater is patterned on the membrane layer, on the opposite side of the wafer from the etch window; typically, 1000 Å of Pt and a 150 Å Ti adhesion layer are used.

After the micro-hot plate is etched and the wafer is diced, the adsorbent ST sol gel layer is applied to the front surface of the micro-hot plate. In most cases, the adsorbent is spray coated, though spin and dip techniques have been evaluated. The final step in assembly is to thermo-ionic bond the Pyrex lid onto the coated micro-hot plate. Together this becomes a preconcentrator.

ADSORPTION

Good performance of the μChemLab™ requires an efficient preconcentrator. The design goal is to capture the maximum amount of analyte from the gas stream within a specific time interval and then release the analyte back into the carrier gas for sensing with minimal dispersion and band spreading. Hence, important factors that need to be considered are:

(a) Maximizing the adsorbent region for collection;

(b) Minimizing the width of the chemical pulse for analysis (ideally < 100 msec);

(c) Minimizing the heating requirement for desorption, that fits within the power budget (i.e. about 100mW at 5V);

(d) Satisfying the short transient time (about 10 msec) to heat the adsorbent bed for desorption.

To guide the design, we have developed an engineering tool to model the mass transfer, adsorption, and desorption process in the preconcentrator. With results obtained from a few exploratory experiments, these critical design parameters that influence the performance of the μChemLab™ have been identified: adsorbent area, coating material, and flow channel geometry, particularly channel height.

Modeling

A major interest in adsorption is to describe the eluted concentration at the preconcentrator exit - the breakthrough curve as a function of time. Predicting the breakthrough curve is a challenging task because adsorption is a transient, highly nonlinear, non-equilibrium physical phenomenon. Modeling includes mass transfer, flow dynamics, surface interactions, and exothermic physicochemical reactions.

Since the present interest is to develop a design tool to evaluate and optimize different preconcentrator designs, a few assumptions are made to simplify the problem and to obtain an analytical solution. These assumptions are as follows:

- Adsorption is irreversible;
- The adsorption isotherm is linear, a reasonable approximation for most adsorbents of interest with low analyte concentrations;
- The effect of the heat of adsorption is minimal;
- Flow in the channel is a 2-D laminar flow with a parabolic velocity profile;
- The analyte concentration on the porous adsorbent surface is relatively uniform; and
- The analyte concentration in the adsorbent can be divided into two regions - a saturation zone and an adsorption zone (Fig. 3). The saturation zone is the region in which the adsorbent bed is in equilibrium with the feed mixture (analyte and carrier gas), and the adsorption zone is the region in which uptake is still occurring.

Prior to the development of a saturation zone at the leading edge of the adsorbent bed, the breakthrough concentration of the analyte can be found by solving the mass transfer equation with a boundary condition assuming a perfect adsorption on the surface.

$$c_{min} = c_o \cdot \exp(-\alpha \cdot l) \quad with \quad \alpha = \frac{kda}{uh} \tag{1}$$

By balancing the amount of analyte being adsorbed and the rate of adsorption, the time required to establish a saturation zone at the front end is:

$$t_{sat} = q_o(1-\varepsilon)/(\alpha \cdot c_o \cdot u \cdot h/d) = q_o(1-\varepsilon)/(k \cdot a \cdot c_o) \tag{2}$$

DISCLAIMER

After the saturation zone is established at the front end of the adsorbent bed, the saturation front begins to propagate steadily across the bed. The speed of the advancing saturation front, u_{sat}, can be determined by balancing the amount of analyte being fed and the amount being adsorbed as

$$u_{sat} = u \cdot c_o / [q_o \cdot (1-\varepsilon)] \quad (3)$$

As the saturation front propagates across the bed, the breakthrough concentration as a function of load time, t, is:

$$c = c_o \cdot \exp\left[-\alpha \cdot \left(l - \frac{u \cdot c_o}{q_o \cdot (1-\varepsilon)} \cdot (t - t_{sat})\right)\right] \quad (4)$$

Comparison with Experiment

In addition to developing a design tool, we have conducted experiments to evaluate different designs and to validate the model. Figure 4 shows a comparison between the predicted and measured breakthrough curve of the adsorption experiment. When adsorption begins at time=*0*, the breakthrough concentration will fall to a minimum value. This minimum concentration will persist until the adsorbent becomes saturated. Then it will slowly increase as the saturation zone starts to propagate across the bed, and eventually returns to its initial value when the bed is fully saturated.

Overall, the analytical model prediction compares reasonably well with experimental data. However a small discrepancy between prediction and data exists. This discrepancy may occur because adsorption is a reversible process while this analytical model assumes the contrary. If modeling a reversible adsorption process, one needs to balance the chemical potential at the adsorbent interface. This will lead to a complicated boundary condition, a highly nonlinear, time-dependent analyte concentration at the adsorbent surface, and a complex solution.

This analytical model also neglects the multi-dimensional geometric effect of fluid and species transport in the flow channel and in the porous sol gel adsorbent. Nevertheless, the comparison shows that this analytical model gives adequate predictions and can be used for design parametric studies, though additional validation against experimental data is highly recommended.

DESORPTION

Modeling

Thermal desorption behaves differently than adsorption; there is no saturation front propagating across the bed. Analyte is being released into the environment caused by a change in the adsorption equilibrium at an elevated temperature. Figure 5 illustrates how the concentration of the analyte adsorbed in the bed changes with temperature, leading to a desorption of the collected sample. In this illustration, a linear adsorption isotherm of the bed is assumed. Initially when the bed becomes saturated (I), the concentration of analyte in the bed and in the gas mixture adjacent to the bed are q_o and c_o , respectively. After the bed is heated up to an elevated temperature (T_2), when desorption begins to take place, the concentration of analyte in the gas mixture adjacent to the adsorbent bed will increase to c_1 (from *I* to *II*). Hence the concentration gradient (c_1 - c_o) is the driving force of diffusion, leading to an increase in the analyte concentration in the carrier gas stream. To simplify our analysis, the present model neglects the existence of a variation in the concentration of analyte across the gas-adsorbent bed interface. At any time during the desorption process (*III*), the concentration of analyte in the bed and in the gas mixture adjacent to the bed are q^* and c^*, respectively. Analyte will be continuously released into the gas stream until the concentration of analyte in the gas mixture adjacent to the bed has fallen back to the c_o level. At this time, the final concentration of the analyte in the bed will be q_f (*IV*). Hence it is very important the transient behavior of the analyte concentration on the surface of the adsorbent bed to be captured throughout the desorption process.

By solving the mass transfer equation with a time-dependent boundary condition, i.e., a transient analyte concentration on the adsorbent surface, the concentration exiting the PC during desorption can be found:

$$c = A(t) \cdot [1 - \exp(-\alpha \cdot l)] + c_o \exp(-\alpha \cdot l) \quad (5)$$

where

$$A(t) = c_1 \cdot \exp(-pt) + c_o \cdot [1 - \exp(-pt)] \quad (6)$$

and

$$p = \frac{ka}{(1-\varepsilon) \cdot (q_o / c_1)} \quad (7)$$

This model predicts that at the beginning of desorption, there will be a sharp spike in the exit concentration. Then the exit concentration will fall exponentially with time. Hence the width of the release pulse is affected by the physical structure of the adsorbent bed, the adsorption isotherm at an elevated temperature, and the mass transfer coefficient. The mass transfer coefficient, subsequently, is a function of flow velocity and channel height.

Comparison with Experiment

The present desorption model needs information regarding the new adsorption isotherm (i.e. q_o / c_1 or q_f / c_o) with respect to the elevated temperature. In order to obtain this new adsorption isotherm, the analyte concentration at the exit of those desorption experiment has been analyzed. By

equilibrating the total amount of analyte being desorbed between prediction and measurement, a new adsorption isotherm can be derived. With this new additional information, the analytical prediction of the analyte concentration at the exit of the PC is compared with the experimental data. Figure 6 shows that this prediction compares reasonably well with the desorption experiment.

The importance of a preconcentrator is demonstrated in the desorption experiment. As illustrated in the figure, the peak concentration of the target analyte is more than two-hundred fold higher than the initial concentration that appears in an ambient condition. In a few other desorption tests, more than four hundred fold increase of peak concentration has been observed [5].

DESIGN EVALUATION

To obtain an excellent performance of the μChemLab™, it is important to design and operate the preconcentrator such that it will collect the maximum amount of the target analyte, then release the total amount for analysis with minimal dilution and dispersion. To achieve this goal, we will next investigate several important physical parameters that can influence the mass transfer, flow rate, adsorption, and desorption in the PC.

Capture Efficiency

Capture efficiency is defined as the percentage of target analyte being adsorbed in the preconcentrator. It reflects the performance of the PC. Figure 7 shows the total amount of analyte that the PC can collect as a function of volumetric flow rate for a given geometry (150 μm high channel) and a fixed collection time.

Results from prediction indicate that the PC can collect a greater amount of target analyte as the volumetric flow rate increases. However the total amount collected will be slowly approaching a maximum value and level off at about 80 mL/min. This finding is predicted by the analytical model and also observed in the experimental data.

Channel Height

The effect of channel height on adsorption and desorption is different. Figure 8 illustrates the effect of different channel heights on adsorption. The breakthrough concentration before saturation is the same for both 36 and 46 μm high channel. The breakthrough value is the same because the volumetric flow rate remains constant in these cases. However the 36 μm channel reaches saturation earlier than the 46 μm channel. This happens because a narrower channel has a better mass transfer rate. (Since the flow in the PC channel is a laminar flow and the Sherwood number for this geometry and under this flow condition is about 4.86, the mass transfer coefficient will be inversely proportional to the channel height.) This finding is also predicted well by the analytical model as given in Equation (2). Similarly, a narrower channel will lead to a faster speed of the saturation front propagating across the adsorbent bed, resulting in a steeper slope of the curve at the latter time. Overall the total amount of analyte collected, which is the integrated area prescribed by the curve, is smaller for the narrower channel. These results show that prediction from the analyte model compares reasonably well with the experimental data.

Figure 9 shows the effect of channel height on desorption predicted by the model. As the channel size decreases, it will generate a shaper pulse. The peak of the concentration curve is much higher and the width at the half-maximum is much narrower. This shape concentration profile will work well for gas chromatography.

The overall effect of channel height on PC performance is not obvious; a narrower channel can be better or worse depending on the conditions. For desorption, it will lead to a shaper pulse. For adsorption, a lesser amount of analyte will be collected, hence the peak height may be smaller. Besides considering analyte collection and release, one needs to be cautious about the drawback of having a too narrow channel. For any mini- or micro-pump of interest, it can only draw a relatively small vacuum pressure, normally at about 6 psia. Hence if the channel size decreases, the flow velocity will decrease at a faster pace. (For a fixed pumping rate, average flow velocity is directly proportional to the square the channel height and the volumetric flow rate is proportional to the fourth power of the channel height.) If the flow velocity becomes very small, a significant dispersion will occur.

Different coating materials

We have investigated the performance of four different kinds of coating materials for adsorption and desorption. They are: 4% hydrophobic CTAB, 10% hydrophobic CTAB, 55% Phenyl, and P123. Figures 10 and 11 show the breakthrough curves of adsorption and desorption for these different adsorbent materials. For analyte collection, the 55% Phenyl coating adsorbs the largest amount of analyte than other coatings (Figure 10). An interesting observation of this set of data: even after 1 minute of adsorption, all the adsorbents have not reached the saturation stage yet.

During desorption, heat is applied to the adsorbent to release the analyte. The measured analyte concentrations at the preconcentrator exit are plotted in figure 11. Desorption result is similar to the adsorption result. Coating with 55% Phenyl, which has the largest amount of analyte being adsorbed, produces the highest peak. For other coating materials, it follows a similar trend, the more analyte being adsorbed, the higher the peak will be. However all the measured peak concentrations are relatively small in this experiment, only a twenty-fold increase of the analyte concentration. More work is underway to improve the adsorbent performance. In addition to the peak height, this analysis also shows that the widths of the half-maximum of the concentration curve for these coating materials are not significantly different. This is fairly consistent to the prediction from the analyte model.

Desorption Temperature

Amongst all the tests analyzed so far, the desorption temperature is constant at 200 degree C. A parameter of interest to improve the performance of the PC is to increase the desorption temperature. At a higher elevated temperature, more target analyte may be released from the adsorbent, but this will require a larger power supply. More desorption occurs because the slope of the adsorption isotherm curve will decrease at a higher temperature. Thus the intermediate point (II) will be shifted further to the right (Fig. 5).

Figure 12 shows the peak concentration as a function of desorption temperature. Between 175 and 225 degree C, the curve is linear. Beyond 225 degree C, the peak concentration will level at about 150. If less than 170 degree C, very little analyte will be desorbed. This implies that the best operation desorption temperature is slightly higher than 200 degree C.

FLOW SIMULATION

The current preconcentrator for the μChemLab™ is assembled together with the micro-hot plate coated on one side with the ST sol gel adsorbent, then covered up with a Pyrex lid that has an inlet and outlet port on the top. A concern with this PC design is that the gaseous flow in the channel may be confined to a narrow region between the inlet and outlet. Thus, some portion of the adsorbent area will not be well exposed to the sample stream, leading to a degraded collection efficiency.

To address this concern, a 3-D computational flow simulation using the MPSalsa code [6] has been performed (Figures 13 and 14). MPSalsa simulation shows the flow across the adsorbent is relatively uniform in the transverse direction. This implies that the whole adsorbent area will be exposed to the sample stream. Hence the capture efficiency for the present PC design should be reasonably good and the assumption of the 2-D flow is valid.

SUMMARY

An adsorption and desorption model for the preconcentrator of the μChemLab™ has been developed. It can be used to perform parametric study for design improvement and optimization. In addition to model development, experiments and computational simulation have been performed to investigate adsorption and desorption in the PC. Results show the model gives reasonably good predictions.

ACKNOWLEDGMENTS

This work is funded by the Laboratory-Directed Research and Development (LDRD) program at Sandia National Laboratories. Sandia is a multiprogram laboratory operated by Sandia Corporation, a Lockheed Martin Company, for the United States Department of Energy under contract number DE-AC04-94AL85000.

REFERENCES

1. Frye-Mason, G. C., Kottenstette, R. J., Heller, E. J., Matzke, C. M., Casalnuovo, S.A., Lewis, P. R., Manginell, R. P., Schubert, W. K., Hietala, V. M., and Shul, R. J., 1998, "Integrated Chemical Analysis System for Gas Phase CW Agent Detection", Micro Total Analysis Systems '98, edited by D. J. Harrison, A. Van Den Berg, Kluwer Academic Publishers, Dordrecht, Netherlands, pp. 477-481.
2. Frye-Mason, G. C., Kottenstette, R. J., Lewis, P. R., Heller, E. J., Manginell, Adkins, D. R., Dulleck, G., Martinez, D., Sasaki, C. Mowry, C. Matzke, and L. Anderson, 2000, "Hand-Held Miniature Chemical Analysis System (μChemlab) for Detection Of Trace Concentrations of Gas Phase Analytes", Micro Total Analysis Systems 2000, Kluwer Academic Publishers, Dordrecht, Netherlands, pp. 229-232.
3. G.T.A. Kovaks, C. W. Storment, and S. P. Kounaves, "Microfabricated Heavy-Metal Ion Sensor", *Sensors and Actuators B, 23*, 41 (1995).
4. C. G. Neuhold, J. Wang, X. H. Cai, and K. Kalcher, "Screen-Printed Electrodes for Nitrite Based On Anion-Exhanger-Doped Carbon Inks", *Analyst, 120,* 2377 (1995).
5. Manginell, P. R., Frye-Mason, G. C., Kottenstette, R. J., and Wong, C. C., 2000, "Microfabricated Planar Preconcentrator," Solid State Sensor and Actuator Workshop, Hilton Head, SC, Transducers Research Foundation, Inc. pp. 179-182.
6. Shadid, J. S., Moffat, H. K., Hutchinson, S. A., Henningan, G. L., Devine, K. D., Salinger, A.G., 1996, "MPSalsa, a Finite Element Computer Program for Reacting Flow Problems, Part 1 - Theoretical Development," *SAND95-2752*, Sandia National Laboratories, New Mexico.

APPENDIX

The governing equation is obtained by satisfying the mass balance between the adsorbent and the gas stream. During adsorption, the analyte transport in the gas stream is:

$$u \cdot \partial c / \partial x = -k \cdot d / h \cdot a \cdot [c - 0]$$

assuming a total analyte adsorption at the surface.

During desorption, the analyte transport in the gas stream is:

$$u \cdot \partial c / \partial x = -(1-\varepsilon) \cdot d / h \cdot \partial q / \partial t$$

For mass transfer within adsorbent, it will be:

$$(1-\varepsilon) \cdot \partial q / \partial t = -k \cdot a \cdot (q / K_2 - c)$$

where K_2 is the new adsorption isotherm (i.e., q_f/c_o).

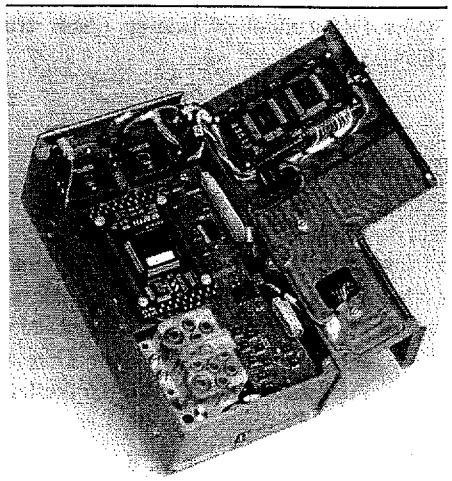

Figure 1 Picture of the μChemLab™, a Hand-held System being Developed for Gas and Liquid Phase Analysis.

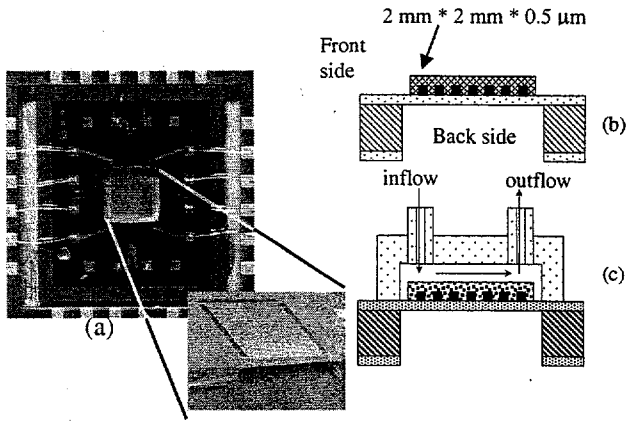

Figure 2 Photograph (a) and Cross-sectional Views of the Preconcentrator without (b) and with (c) a Flow Channel.

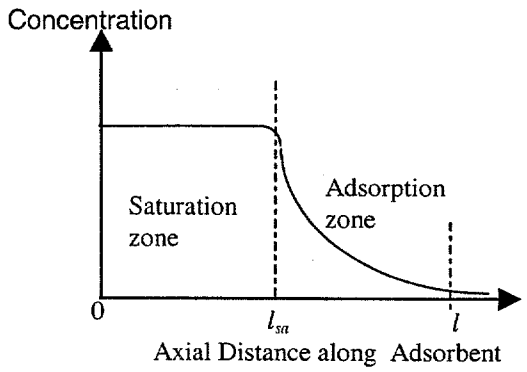

Figure 3 Schematic Diagram of Analyte Distribution in the Preconcentrator Adsorbent.

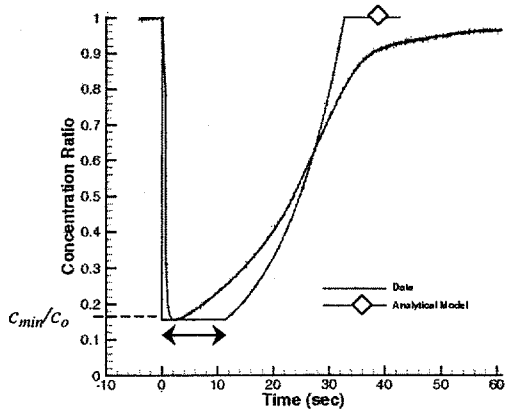

Figure.4 Comparison of the Predicted and Measured Breakthrough Curve for an Adsorption Experiment.

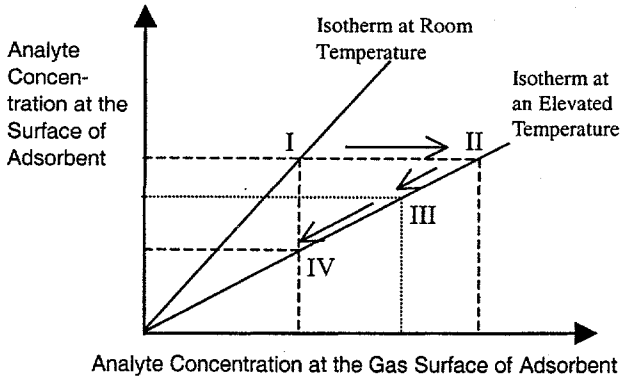

Figure 5 Behavior of Adsorption Isotherms at Different Temperatures to Illustrate the Thermal Desorption Process (I→II→III→IV).

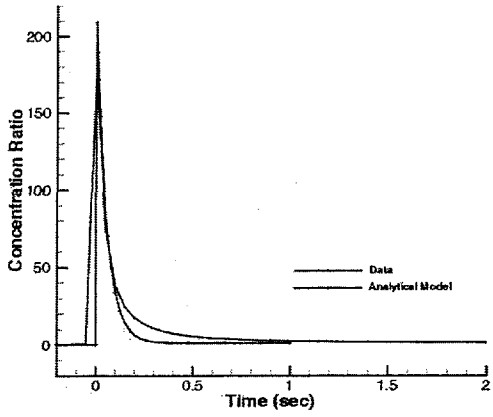

Figure 6 Comparison between the Predicted and Measured Analyte Concentration at the Exit of the Adsorbent for a Desorption Test.

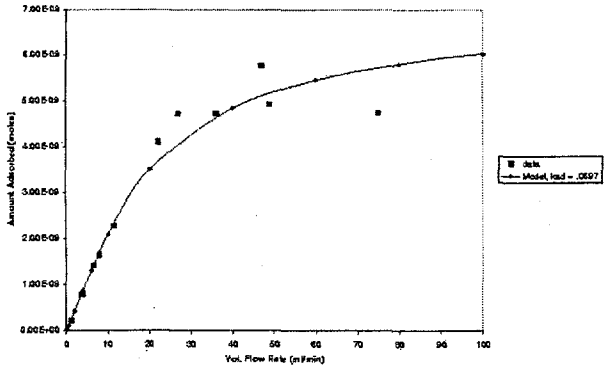

Figure 7 Total Amount of Analyte Collected for Different Volumetric Flow Rates (Prediction versus Measurement).

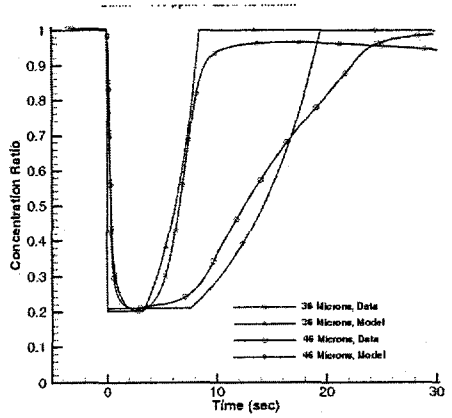

Figure 8 Effect of Channel Height on Adsorption (Predictions versus Data for 2 Different Channel Heights, V-dot=4.5 mL/min).

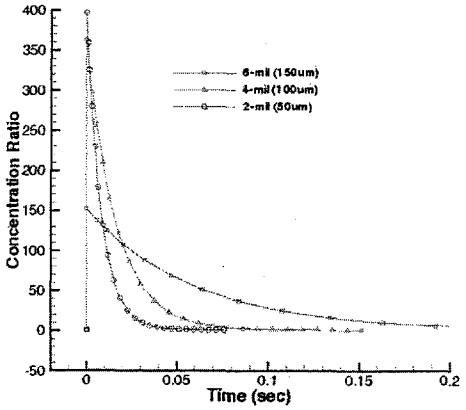

Figure 9 Effect of Channel Height on the Analyte Concentration at the Exit of the Adsorbent during Desorption (Model Prediction).

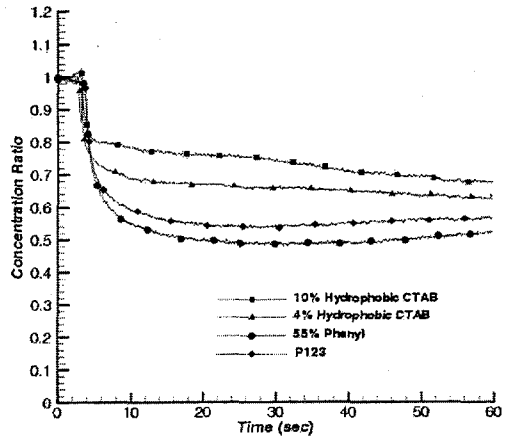

Figure 10 Effect of Different Coating Materials on Adsorption

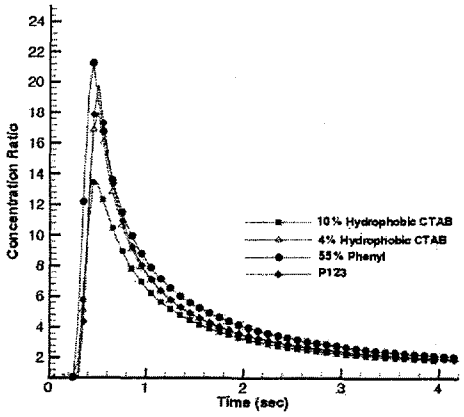

Figure 11 Effect of Different Coating Materials on Desorption

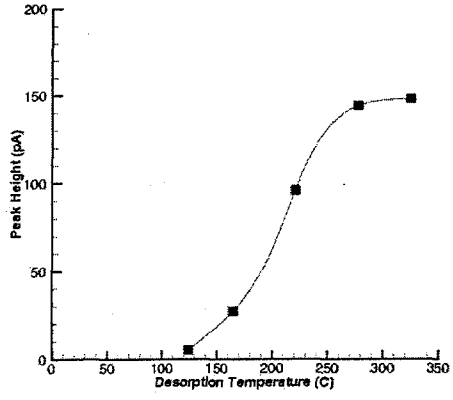

Figure 12 Effect of Adsorbent Temperature on Desorption.

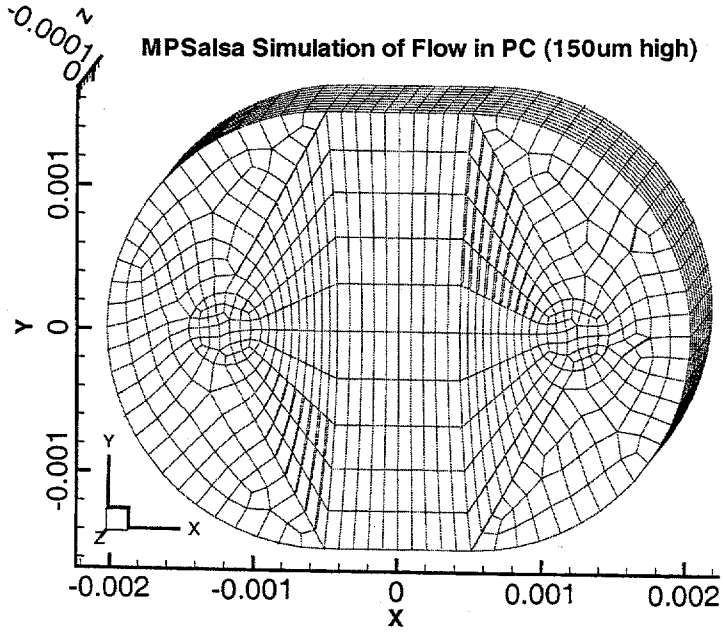

Figure 13 Computational Mesh Layout for 3-D Flow Simulation.

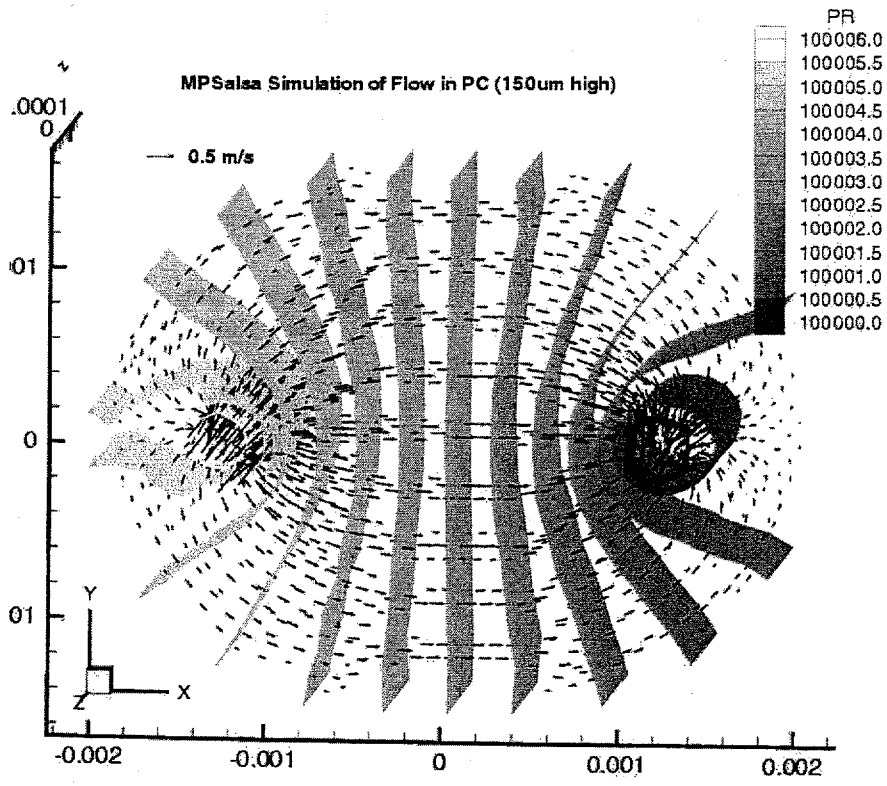

Figure 12 Velocity and Pressure Distribution in the PC Flow Channel Simulated by the MPSalsa Code. (Top View; Flow proceeds from the Left to the Right.)